Proceedings of the World Congress on Engineering 2012 Vol I
WCE 2012, July 4 - 6, 2012, London, U.K.

Hydromagnetic Pulsating Flow of Blood in a Constricted Porous Channel: A Theoretical Study

G. C. Shit and M. Roy

***Abstract*—A theoretical study of pulsatile blood flow through a constricted porous channel in the presence of an external magnetic field by considering the incompressible Newtonian fluid model is investigated. The influence of magnetic field on the flow is studied using the dimensionless magnetic parameter M and a Darcian linear impedance for low Reynolds number is taken into account in the transformed momentum equation. A perturbation method is employed to solve the governing differential equations by using a small perturbation parameter ϵ (such that $0 < \epsilon << 1$), which is incorporated in the time dependent transpiration velocity (suction/ injection). Using appropriate boundary conditions analytical expressions for the velocity distribution, volumetric flow rate and wall shear stress have been derived and the numerical results are presented graphically for different values of the physical parameters of interest.**

***Index Terms*—Pulsatile flow, porous channel, Time dependent suction/ injection**

I. Introduction

MATHEMATICAL modeling of blood flow through a constricted porous channel/ vessel is of great concerned for clinical scientists and has therefore drawn serious attention of researchers. It is known that stenosis (narrowing of artery) is a dangerous disease and is caused due to the deposition of cholesterol and other various substances in an arterial wall form a plaque which grow inward and restrict the flow of blood through the lumen of the artery. If this disease takes a severe form, it may lead to morbidity, fatality and serious circulatory disorders. As a result of such undesirable formation at the endothelium of the vessel wall, reduction of regular blood flow is likely to take place in the constricted region of the channel/vessel. To understand the effects of stenosis in the lumen of an artery, many researchers ([8], [4] and [11]) have investigated the flow of blood through arteries by considering blood as a Newtonian fluid. However, most of the studies ([13], [26] and [12]) show that, in the vicinity of a stenosis, the shear rate of blood is low and the blood behaves like a non-Newtonian fluid. It is also worth while to mention here that although blood is non-Newtonian suspension of cells in plasma, [8] remarked that for vessels of radius greater than 0.025 cm, blood may be considered as a homogeneous Newtonian fluid. Several studies ([21], [27] and [5]) of physiological fluid dynamics through stenosed arteries have been carried out to evaluate the flow pattern under steady and pulsatile conditions by treating blood as a Newtonian fluid.

It has been observed that blood flow in the human circulatory system depends upon the pumping action of the heart, which in turn produces a pulsatile pressure gradient throughout the system. [26] theoretically analyzed the pulsatile flow of blood in a stenosed artery, where the non-Newtonian behavior of blood was taken to be of Herschel-Bulkley type. Some excellent studies on pulsatile blood flow have made by [29]. [30] studied the fluid dynamics of pulsatile flow past a single cylinder for a non-Newtonian Casson fluid. [10] carried out the pulsatile flow of blood in an artery by considering the effects of body acceleration. [23] modeled the blood flow through arterial stenosis by treating blood as a couple stress fluid. [22] proposed a mathematical model for pulsatile blood flow in a constricted tube using the Power-law fluid. The effect of externally imposed body acceleration and magnetic field on peristaltic flow of blood through an arterial segment having stenosis has been investigated by [25]. Their studies pertains to a situation in which blood obeying micropolar fluid model, where the effect of heat transfer phenomena has been taken into account.

In the recent past, engineers and scientists became interested in the influence of magnetic field on blood flows with a view to utilizing MHD (magnetohydrodynamic) in controlling blood flow during surgery and also establishing the effects of magnetic field on blood flows in astronauts, citizens living in the vicinity of electromagnetic towers etc. Since blood consists of a suspension of red blood cells containing hemoglobin, which contains iron oxide, it is quite apparent that blood is electrically conducting and exhibits magnetohydrodynamic flow characteristics. Bhargava et al [1] numerically studied the pulsatile flow and mass transfer of an electrically conducting Newtonian biofluid via a channel with porous medium. The flow of blood through arteries in the presence of magnetic field under different physiological conditions were reported in ([16], [20]). Steady laminar flow of blood through a porous medium in an arterial segment having double stenoses under the influence of externally applied magnetic field have been carried out by [17], [18] using numerically as well as analytically by means of Frobenius Method. The potential use of such MHD principles in various arteries have explored by [14], [15], who showed that for unsteady flow of blood in an artery of circular cross-section, a uniform magnetic fields alters the flow rate of blood. [24] have investigated using a vorticity formulation of the MHD oscillatory flows in variable cross-sectional channels, reporting a distinct reduction in velocity with a strong applied magnetic field. Many biological tissues such as bones and vascular tissues, the renal system as well as the blood vessels containing fatty deposits are assumed to be porous by nature. [7] have presented a detailed review on heat and fluid flow in a porous media having physiological applications. Pulsatile flow of blood through a stenosed porous medium has been studied by [3] under the influence of body acceleration.

Manuscript received March 22, 2012; accepted April 09, 2012. One of the authors G. C. Shit is thankful to the UGC, New Delhi for the financial support during this investigation through UGC Minor Research Project Scheme.
G. C. Shit and M. Roy are with the Department of Mathematics, Jadavpur University, Kolkata-700032, India, E-mail: gcs@math.jdvu.ac.in.

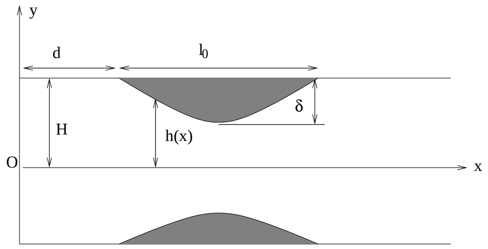

Fig. 1. A schematic diagram of the problem

Very recently [9] theoretically studied the pulsating flow of a hydromagnetic fluid between permeable beds while, [28] have analyzed same problem without considering the effects of magnetic field.
In the present paper, we have investigated the steady as well as transient flow regime for Newtonian hydromagnetic blood flow in a constricted porous channel. The study pertains to a situation where a magnetic field is applied in a direction transverse to the direction of flow. Of specific interest is to determine the velocity profile, the variation of skin-friction and the flow rate with axial distance and with time for different values of the magnetic number, Reynolds number and Darcian porous parameter as well as for different depths of the constriction. The study also bears a potential useful for evaluating the role of porosity of the constricted channel wall.

II. Formulation of the Problem and its Solution

Let us consider the flow of blood in laminar, incompressible, magnetohydrodynamic and pulsatile flow through a two- dimensional constricted channel with porous walls containing a non-Darcian porous material. The channel walls are located at a distance $2H$ apart with reference to a cartesian coordinate system (x, y, t), where x defines the longitudinal coordinate in the direction of flow, y be the transverse coordinate perpendicular to x and t being time. A uniform magnetic field of strength B_0 is applied transverse to the flow direction (cf. Fig. 1). The governing equations for the pulsating porous hydromagnetic flow of blood by neglecting induced magnetic field are taken to be

$$\frac{\partial u}{\partial x} + \frac{\partial v}{\partial y} = 0, \tag{1}$$

$$\frac{\partial u}{\partial t} + u\frac{\partial u}{\partial x} + v\frac{\partial u}{\partial y} = -\frac{1}{\rho}\frac{\partial p}{\partial x} + \nu\left(\frac{\partial^2 u}{\partial x^2} + \frac{\partial^2 u}{\partial y^2}\right) - \frac{\sigma B_0^2}{\rho}u - \frac{\nu}{k}u, \tag{2}$$

$$\frac{\partial u}{\partial t} + u\frac{\partial v}{\partial x} + v\frac{\partial v}{\partial y} = -\frac{1}{\rho}\frac{\partial p}{\partial y} + \nu\left(\frac{\partial^2 v}{\partial x^2} + \frac{\partial^2 v}{\partial y^2}\right). \tag{3}$$

where (u, v) denotes the velocity components along x and y direction respectively, p the fluid pressure, ν the kinetic viscosity, σ the electrical conductivity, B_0 the strength of uniform magnetic field and k denotes the permeability of porous medium.
We assume that the fluid is injected/ sucked off through the channel walls with a time dependent velocity V is given by ([20])

$$V = V_0\left(1 + \epsilon A e^{i\omega t}\right) \tag{4}$$

Where V_0 be the uniform transpiration velocity (for injection $V_0 > 0$ and for suction $V_0 < 0$) and the product ϵA is necessarily less than unity.
We also assume that the length of the constricted channel is much greater than the height of the channel. Since the fluid medium is filled with porous material and the normal component of velocity $v = V$ is independent of x and y and thereby continuity equation (1) reduces to $\frac{\partial u}{\partial x} = 0$. Therefore, taking into consideration that the fluid flow takes place only along the axis of the channel and denoting the velocity by u, where $u = u(y, t)$ and then the equation (3) simply reduces to $\frac{\partial p}{\partial y} = 0$.
Owing to the above mentioned assumptions the axial momentum equation reduces to

$$\frac{\partial u}{\partial t} + V_0\left(1 + \epsilon A e^{i\omega t}\right)\frac{\partial u}{\partial y} = -\frac{1}{\rho}\frac{\partial p}{\partial x} + \nu\frac{\partial^2 u}{\partial y^2} - \frac{\sigma B_0^2}{\rho}u - \frac{\nu}{k}u \tag{5}$$

Since the fluid is driven by the pumping action of the heart, which in turn produces a pulsatile pressure gradient and can be approximated as

$$-\frac{\partial p}{\partial x} = P_s + \epsilon P_0 cos(\omega t), \tag{6}$$

where P_0 and P_s are the pulsatile amplitude and steady component of the pressure gradient respectively.
The geometry of the stenosis which is assumed to be symmetric is given by

$$\begin{aligned} h'(x) &= H\left[1 - \frac{\delta}{2}\left\{1 + cos\frac{2\pi}{l_0}\left(x - d - \frac{l_0}{2}\right)\right\}\right]a(t), \quad d \le x \le d + l_0, \\ &= Ha(t), \qquad otherwise \end{aligned} \tag{7}$$

in which,

$$a(t) = 1 - \{cos(2\pi T) - 1\}ke^{-2\pi kT}.$$

where δ be the depth/ height of the stenosis, l_0 be the length of the stenosis, d be the distance of onset of the stenosis from the y- axis, $h(x)$ be the variable height of the channel at the stenosed portion, T the non-dimensional time and k denotes the amplitude of oscillation.
Considering the flow to be symmetric about the center line $y = 0$ of the channel, we focus our attention to the flow in the region $0 \le y \le h(x) = \frac{h'(x)}{H}$ only.
The corresponding boundary conditions are prescribed as follows:

$$u = 0 \qquad at \qquad y = h(x), \tag{8}$$

$$\frac{\partial u}{\partial y} = 0 \qquad at \qquad y = 0 \tag{9}$$

Let us introduce the following non-dimensional variables

$$u^* = \frac{u}{V_0}, \quad y^* = \frac{y}{H}, \quad x^* = \frac{x}{H}, \quad T = \frac{\omega}{2\pi}t, \quad p^* = \frac{p}{\rho V_0^2},$$

$$\tau_{xy}^* = \frac{\mu V_0}{H}\tau_{xy}$$

ISBN: 978-988-19251-3-8
ISSN: 2078-0958 (Print); ISSN: 2078-0966 (Online)

Using these dimensionless variables in equation (5) and dropping asterisks, we obtain

$$\frac{\alpha^2}{2\pi Re}\frac{\partial u}{\partial T}+\left(1+\epsilon A e^{i2\pi T}\right)\frac{\partial u}{\partial y}=-\frac{\partial p}{\partial x}+\frac{1}{Re}\frac{\partial^2 u}{\partial y^2}-\left(M+\frac{1}{\lambda}\right)u \quad (10)$$

where

$$\alpha=H\sqrt{\frac{\omega}{\nu}},\quad Re=\frac{HV_0}{\nu},\quad M=\frac{\sigma B_0^2 H}{\rho V_0}\quad and \quad \lambda=\frac{kV_0}{\nu H}$$

We assume that the solution of the flow problem takes in the following form

$$u(y,T)=u_0(y)+\epsilon u_1(y)e^{i2\pi T} \quad (11)$$

where u_0 and u_1 are the velocity of steady state and transient state respectively.
Substituting (11) into the equations (8) - (10) we obtain the differential equations along with the boundary conditions in steady state and transient state as follows:
(i) Steady state:

$$\frac{1}{Re}\frac{d^2u_0}{dy^2}-\frac{du_0}{dy}-\left(M+\frac{1}{\lambda}\right)u_0=-P_s \quad (12)$$

$$u_0=0 \qquad on \qquad y=h(x), \quad (13)$$
$$\frac{du_0}{dy}=0 \qquad on \qquad y=0.$$

(ii) Transient state:

$$\frac{1}{Re}\frac{d^2u_1}{dy^2}-\frac{du_1}{dy}-\left(M+\frac{1}{\lambda}+\frac{i\alpha^2}{Re}\right)u_1=A\frac{du_0}{dy}-P_0\cos(2\pi T)e^{-2i\pi T} \quad (14)$$

$$u_1=0 \qquad on \qquad y=h(x), \quad (15)$$
$$\frac{du_1}{dy}=0 \qquad on \qquad y=0.$$

Now, by solving equations (12) and (14) subject to the boundary conditions (13) and (15) we obtain

$$u_0=C_1e^{\lambda_1 y}+C_2e^{\lambda_2 y}+E \quad (16)$$

and

$$u_1=C_3e^{\lambda_3 y}+C_4e^{\lambda_4 y}+F_1e^{\lambda_1 y}+F_2e^{\lambda_2 y}+F_3 \quad (17)$$

where $C_1,\ C_2,\ C_3,\ C_4,\ \lambda_1,\cdots$ etc. given in the appendix. Substituting the expressions of u_0 and u_1 from equations (16) and (17) in (11), we obtain an expression for the velocity $u(y,T)$ as

$$u(y,T)=\left(C_1e^{\lambda_1 y}+C_2e^{\lambda_2 y}+E\right)+\left[C_3e^{\lambda_3 y}+C_4e^{\lambda_4 y}+F_1e^{\lambda_1 y}+F_2e^{\lambda_2 y}+F_3\right]\epsilon e^{i2\pi T} \quad (18)$$

After having determine u, one can obtain the volumetric flow rate Q, defined by

$$Q=\int_0^{h(x)}u(y,T)dy \quad (19)$$

which on integration yields

$$Q=\left(C_1T_1+C_2T_2+Eh(x)\right)+\epsilon e^{i2\pi T}\left(C_3T_3+C_4T_4+T_1F_1+T_2F_2+F_3h(x)\right) \quad (20)$$

The non-dimensional wall shear stress is given by the relation

$$\tau_w=\left[\frac{\partial u}{\partial y}\right]_{y=h(x)} \quad (21)$$

Use of (18) in equation (21), the wall shear stress can be written as

$$\tau_w=\left(C_1\lambda_1e^{\lambda_1 h(x)}+C_2\lambda_2e^{\lambda_2 h(x)}\right)+\epsilon e^{i2\pi T}\big(C_3\lambda_3e^{\lambda_3 h(x)}+C_4\lambda_4e^{\lambda_4 h(x)}+F_1\lambda_1e^{\lambda_1 h(x)}+F_2\lambda_2e^{\lambda_2 h(x)}\big) \quad (22)$$

III. Results and Discussion

The primary object of this investigation has been to study the flow of blood in a constricted porous channel subject to the pulsatile pressure gradient in the presence of an applied magnetic field, where the transpiration velocity assumed to be periodic. The analytical expressions for velocity distribution, volumetric flow rate and the wall shear stress have been derived in the previous section and are computed numerically by taking into account the real part of such expressions. The numerical solutions have been illustrated based upon the following data with non-dimensional form available in the scientific literatures ([30], [1], [19] and [2]): $Re = 1,\ 5,\ 10,\ 15;\quad \alpha = 0.5,\quad A = 2,\ 5;\quad \epsilon = 0.01,\ \ P_0 = 7,\ \ P_s = 10,\ \ M = 0,\ 2,\ 4,\ 6; k = 0.01,\ \lambda = 0.1,\ 0.3,\ 0.5,\ 1.0;\quad L = 5.0$. The study of [6] reported an analysis of the pressure changes in the vessels of human vascular under the action of a strong magnetic field within a range of 2.3 to 4.7 Tesla. In all numerical computations, the solutions have been obtained for the general case by adopting a particular time T=1.0. The blockage of the channel was examined in three different cases, by taking $\delta = 0.10$, $\delta = 0.25$ and $\delta = 0.50$. These three values were taken to present respectively the mild and moderate stages of the channel constriction. In the flow geometry of the channel, $x = d + \frac{l_0}{2}$ indicates the position at the maximum depth of the constriction called throat of the stenosis.
Figs. 2-6 give the variation of pulsating axial velocity along with the dimensionless transverse coordinate for different values of the physical parameters. It reveals from Fig. 2 that the axial velocity decreases with the increase of the magnetic field strength. It indicates that the blood velocity can be reduced upto 20% - 30% by applying sufficient strength of magnetic field. Thus the results for a reduction in blood velocity can be used for surgical patient during surgery. While the reversal trend is occurring in Fig. 3, which depicts the influence of porosity on the axial velocity u. It has been observed that increasing values of λ corresponds to a rise in permeability and therefore, physically implies that the permeating fluid receives less resistance to flow.

It is interesting to note from Fig. 4 that maximum velocity occurs at the central line of the channel for all values of the Reynolds number Re, however in the vicinity of the channel wall the velocity increases with the increase of the Reynolds numbers Re. From this figure it is interesting to note that no change is observed in the axial velocity at the central region of the channel for Reynolds number $Re > 3$. Figs. 5 and 6 represent the velocity profiles at different locations of the channel constriction as well as for different depths. Fig. 5 depicts that the axial velocity strongly decreases near the

ISBN: 978-988-19251-3-8
ISSN: 2078-0958 (Print); ISSN: 2078-0966 (Online)

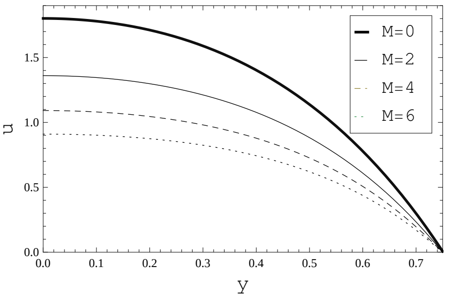

Fig. 2. Axial velocity profiles with dimensionless transverse coordinate at the throat of the stenosis for different values of the magnetic number$M$, when $Re = 1, \alpha = 0.5, T = 1.0, \lambda = 0.3, \delta = 0.25$

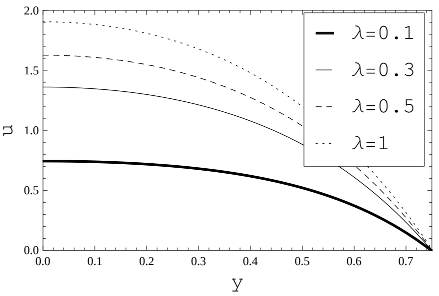

Fig. 3. Axial velocity profiles with dimensionless transverse coordinate at the throat of the stenosis for different values of the Darcian porosity parameter λ when $Re = 1, \alpha = 0.5, T = 1.0, M = 2, \delta = 0.25$

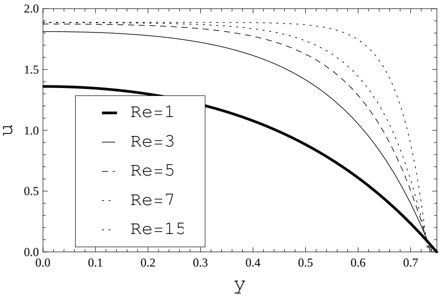

Fig. 4. Variation of axial velocity for different Reynolds number with $\alpha = 0.5, T = 1.0, \lambda = 0.3, \delta = 0.25, M = 2$

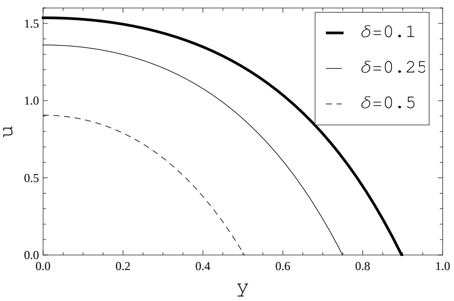

Fig. 5. Variation of velocity profile at different depth of the stenosis with $Re = 1, \alpha = 0.5, T = 1.0, \lambda = 0.3, M = 2$

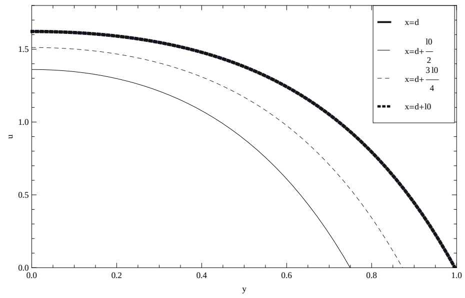

Fig. 6. Variation of velocity profile at different location of the stenosis with $Re = 1, \alpha = 0.5, T = 1.0, \lambda = 0.3, M = 2, \delta = 0.25$

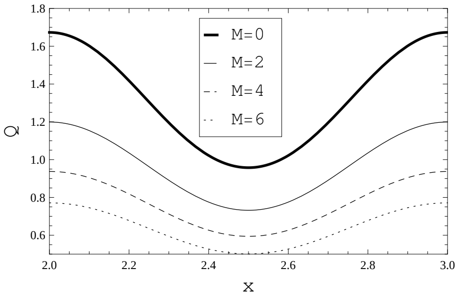

Fig. 7. Variation of volumetric flow rate along with the axial distance for different magnetic number M, when $Re = 1, A = 2, \alpha = 0.5, T = 1.0, \lambda = 0.3, \delta = 0.25$

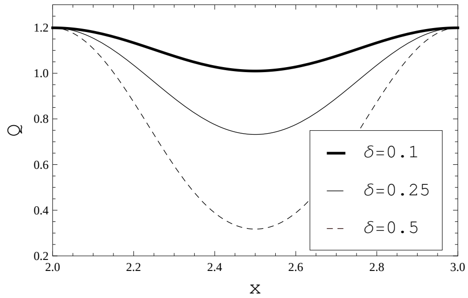

Fig. 8. Variation of volumetric flow rate for different height of the stenosis with $Re = 1, A = 2, \alpha = 0.5, T = 1.0, \lambda = 0.3, M = 2$

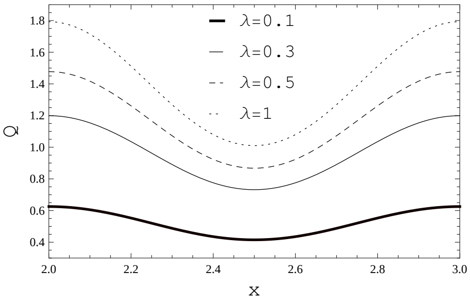

Fig. 9. Variation of volumetric flow rate along the longitudinal distance for different porosity parameter λ, with $Re = 1, A = 2, \alpha = 0.5, T = 1.0, \delta = 0.25, M = 2,\ x = d + \frac{l_0}{2}$

channel wall as well as in the central line of the channel with the increasing effects of constriction height. While from Fig. 6 we observe that the velocity is least at the throat of the stenosis and is maximum at the onset as well as outset of the stenosis.

The variation in volumetric flow rate of blood is illustrated through Figs. 7-9 along the longitudinal distance of the channel. The rate of blood flow has reducing effect with the increasing magnetic field strength. The flow rate is also found to be minimum in all cases at the throat of the stenosis.

One can further note that the volumetric flow rate decreases with the height of the stenosis and increases with the increase of the Darcian porosity parameter λ. Figs. 10 and 11

ISBN: 978-988-19251-3-8
ISSN: 2078-0958 (Print); ISSN: 2078-0966 (Online)

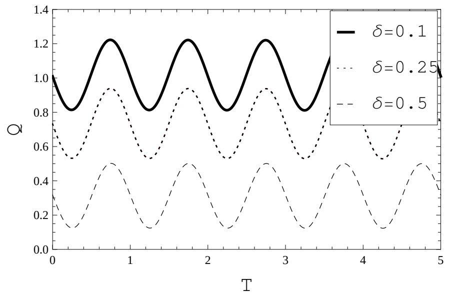

Fig. 10. Variation of volumetric flow rate with time for different height of the stenosis δ, when $Re = 1, A = 2.0, \alpha = 0.5, T = 1.0, \lambda = 0.3, M = 2,\ x = d + \frac{l_0}{2}$

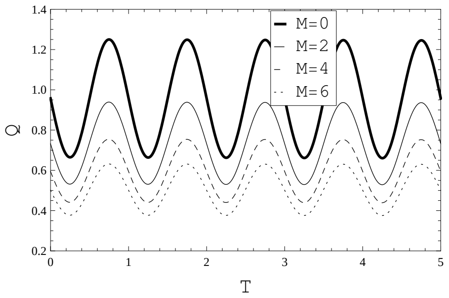

Fig. 11. Variation of volumetric flow rate with time for different magnetic number M, when $Re = 1, A = 2, \alpha = 0.5, \delta = 0.25, \lambda = 0.3$

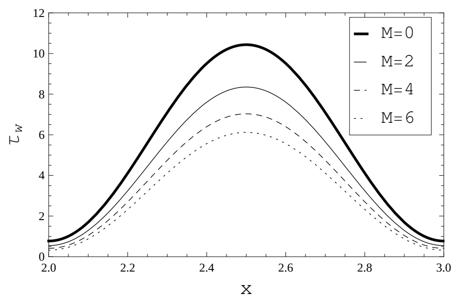

Fig. 12. Distribution of wall shear stress for different values of the magnetic number M, when $Re = 10, \alpha = 0.5, A = 5, \lambda = 0.3, T = 0.5, \delta = 0.25$

give the variation of volumetric flow rate with time in cycle. The volumetric flow rate is found to oscillates periodically with time and the magnitude of the flow rate decreases with the increase of the magnetic number M. It is also reveal that for a high value of Reynolds number as well as for severe stages of the channel constriction the volumetric flow rate becomes negative and hence physically implies that at high Reynolds number vorticity may appear at the downstream of the stenosis. Although our study is based on the mild stenosis and for low Reynolds number, consideration of unidirectional flow may valid.

The distribution of wall shear stress along the axial distance as well as for time in cycle for different values of the rheological parameters are shown in Figs 12-16. It is well known that, when the shear stress generated on the wall is high, the vessel wall may be damaged, leading to the intimal thickening. While in the case of low shear stress at the wall, mass transportation takes place, giving rise to deposition of cholesterol and other substances. It should be noted from Fig. 12 that wall shear stress decreases as the values of M increases, while from Fig. 13 that the wall shear stress

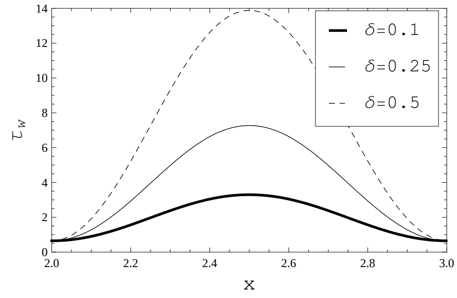

Fig. 13. Distribution of wall shear stress for different height of the stenosis with $Re = 10, \alpha = 0.5, A = 5, \lambda = 0.3, T = 0.5, M = 2$

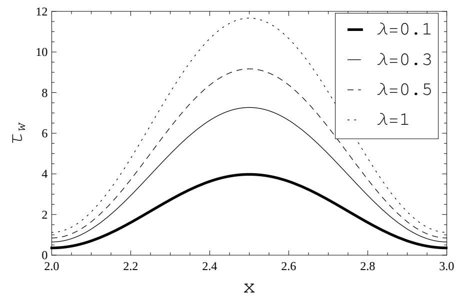

Fig. 14. Distribution of wall shear stress along the length of the stenosis for different λ with $Re = 10, \alpha = 0.5, A = 5, M = 2, T = 0.5, \delta = 0.25$

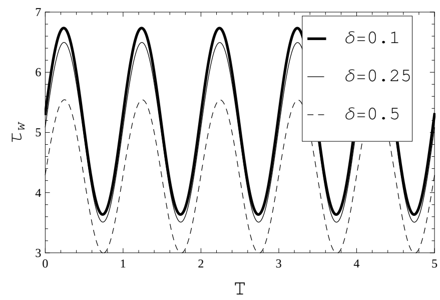

Fig. 15. Variation of wall shear stress with time for different depth of the stenosis when $Re = 10, \alpha = 0.5, A = 5, \lambda = 0.3, M = 2$

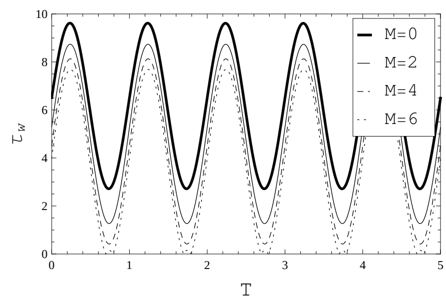

Fig. 16. Variation of wall shear stress with time for different values of the magnetic number M, when $Re = 5, A = 5, \alpha = 0.5, T = 0.5, \lambda = 0.3, M = 5, \delta = 0.25$

increases with the increase of the stenosis height.

It is interesting to note from Fig. 14 that the Darcian parameter λ has an enhancing effect on the wall shear stress.

Results presented in Figs. 15 and 16 show that the wall shear stress oscillates periodically with time and that the magnitude of the wall shear stress decreases with the increase in the stenosis depth δ and magnetic parameter M.

ISBN: 978-988-19251-3-8
ISSN: 2078-0958 (Print); ISSN: 2078-0966 (Online)

IV. CONCLUSION

In the present theoretical study, an attempt has been made to examine the effects of low Reynolds number, Darcian porosity parameter and an external magnetic field on pulsating blood flow in a constricted channel by assuming time dependent transpiration velocity. The detailed illustration of the flow characteristics have been made numerically to perform some graphical presentation of the computed results. The study shows that the instantaneous flow characteristics are significantly affected by magnetic number, porosity parameter as well as by Reynolds number. It reveals that increasing magnetic field serves to reduce blood flow and increase in Reynolds number as well as porosity parameter increases the flow velocity. The increasing values of the constriction height has an enhancing effect on the wall shear stress and has reducing effect on the volumetric flow rate of blood. It further reveals that by the application of an external magnetic field bears the potential to reduce the flow of blood, wall shear stress and the volumetric flow rate. On the basis of the present results, it can be concluded that the flow of blood can be controlled by the application of sufficiently strong magnetic field. Thus, this investigation throws towards the application in clinical treatment of haemodynamic diseases such as hypertension and atherosclerosis.

APPENDIX A

$$C_1 = \frac{E\lambda_2}{\lambda_1 e^{\lambda_2 h(x)} - \lambda_2 e^{\lambda_1 h(x)}}, \quad C_2 = -\frac{\lambda_1}{\lambda_2}C_1, \quad E = \frac{P_s}{M+\frac{1}{\lambda}},$$
$$\lambda_1 = 0.5\left(Re + \sqrt{Re^2 + 4Re\left(M + \frac{1}{\lambda}\right)}\right),$$
$$\lambda_2 = 0.5\left(Re - \sqrt{Re^2 + 4Re\left(M + \frac{1}{\lambda}\right)}\right)$$
$$\lambda_3 = 0.5\left(Re + \sqrt{Re^2 + 4Re\left(M + \frac{1}{\lambda} + \frac{i\alpha^2}{Re}\right)}\right),$$
$$\lambda_4 = 0.5\left(Re - \sqrt{Re^2 + 4Re\left(M + \frac{1}{\lambda} + \frac{i\alpha^2}{Re}\right)}\right),$$
$$C_3 = \frac{C_{31}+C_{32}+F_3\lambda_4}{\left(\lambda_3 e^{\lambda_4 h(x)} - \lambda_4 e^{\lambda_3 h(x)}\right)}, \quad C_{31} = F_1\lambda_4 e^{\lambda_1 h(x)} - \lambda_1 e^{\lambda_4 h(x)},$$
$$C_{32} = F_2\lambda_4 e^{\lambda_2 h(x)} - \lambda_2 e^{\lambda_4 h(x)}, \quad C_4 = -\frac{(F_1\lambda_1 + F_2\lambda_2 + C_3\lambda_3)}{\lambda_4},$$
$$F_1 = \frac{AReC_1\lambda_1}{D_1}, \quad F_2 = \frac{AReC_2\lambda_2}{D_2}, \quad F_3 = \frac{P_0 cos(2\pi T)e^{-2\pi iT}}{\left(M+\frac{1}{\lambda}+\frac{i\alpha^2}{Re}\right)}$$
$$D_1 = \lambda_1^2 - \lambda_1 Re - Re\left(M + \frac{1}{\lambda} + \frac{i\alpha^2}{Re}\right),$$
$$D_2 = \lambda_2^2 - \lambda_2 Re - Re\left(M + \frac{1}{\lambda} + \frac{i\alpha^2}{Re}\right)$$
$$T_1 = \frac{e^{\lambda_1 h(x)}-1}{\lambda_1}, \quad T_2 = \frac{e^{\lambda_2 h(x)}-1}{\lambda_2},$$
$$T_3 = \frac{e^{\lambda_3 h(x)}-1}{\lambda_3}, \quad T_4 = \frac{e^{\lambda_4 h(x)}-1}{\lambda_4},$$

REFERENCES

[1] R. Bhargava, S. Rawat and H. S. Takhar, "Pulsatile magneto-biofluid flow and mass tansfer in a non-Darcian porous medium channel," *Meccanica*, vol. 42, pp. 247-262, 2007.
[2] K. Y. Chan, H. Fujioka, R. H. Bertlett, R. B. Hirschl and J. B. Grotberg, J. B., "Pulsatile flow and mass transfer over an array of cylinders: Gas transfer in a cardiac-driven artificial lung," *J. Biomech. Engg.*, vol. 128, pp. 85–96, 2006.
[3] M. El-Shahed, "Pulsatile flow of blood through a stenosed porous medium under periodic body acceleration," *Appl. Math. Comput.*, vol. 138, pp. 479 - 488, 2003.
[4] J. H. Forrester and D. F. Young, "Flow through a converging and diverging tube and the implication in occlusive vascular disease," *J. Biomech.*, vol. 3, pp. 297–316, 1970.
[5] T. K. Hung and M. C. Tsai, "Kinematic and dynamic characteristics of pulsatile flows in stenotic vessels," *ASCE J. Engg. Mech.*, vol. 123 pp. 247–259, 1997.
[6] J. R. Keltner, M. S. Roos, P. R. Brakeman and T. F. Budinger, "Magnetohydrodynamics of blood flow," *Mag. Reson. Med. J.*, vol. 16, pp. 139–149, 1990.
[7] A. R. Khaled and K. Vafai, "The role of porous media in modelling flow and hear transfer in biological tissues," *Int. J. Heat and Mass Trans.*, vol. 46, pp. 4989 - 5003, 2003.
[8] D. A. MacDonald, "On steady flow through modeled vascular stenosis," *J. Biomech.*, vol. 12, pp. 13-20, 1979.
[9] T. Malathy and S. Srinivas, "Pulsating flow of a hydromagnetic fluid between permeable beds," *Int. Commun. Heat and Mass Transf.*, vol. 35, pp. 681-688, 2008.
[10] M. Massoudi and T. X. Phuoc, "Pulsatile flow of blood using a modified second-grade fluid model," *Comput. Math. Applic.*, vol. 56, pp. 199-211, 2008.
[11] J. C. Misra and S. Chakravarty, "Flow in arteries in the presence of stenosis," *J. Biomech.*, vol. 19, pp.907–918, 1986.
[12] J. C. Misra and S. K. Ghosh, "A mathematical model for the study of Inerstial fluid movement vis-a-vis the non-Newtonian behaviour of blood in a constricted artery," *Comput. Math. Applic.*, vol. 41, pp. 783-811, 2001.
[13] J. C. Misra and G. C. Shit, "Blood flow through arteries in a pathological state- A theoretical study," *Int. J. Engg. Sci.*, vol. 44, pp. 662-671, 2006.
[14] J. C. Misra and G. C. Shit, "Effect of magnetic field on blood flow through an artery: A numerical model," *Computational Technologies*, vol. 12 no 4, pp. 3-16, 2007.
[15] J. C. Misra and G. C. Shit, "Flow and Heat transfer of a MHD viscoelastic fluid in a channel with stretching walls: Some applications to haemodynamics," *Computers & Fluids*, vol. 37 pp. 1-11, 2008.
[16] J. C. Misra, B. Pal and A. S. Gupta, "Hydromagnetic flow of a second-grade fluid in a channel - some applications to physiological systems," *Math. Model. Methods in Appl. Sci.*, vol. 8, pp. 1323-1342, 1998.
[17] J. C. Misra, A. Sinha and G. C. Shit, "A numerical method for the magnetohydrodynamic flow of blood in a porous channel," *J. Mech. Med. Biol.*, vol. 11, pp. 547-562, 2011a.
[18] J. C. Misra, A. Sinha and G. C. Shit, "Mathematical modeling of blood flow in porous vessels having double stenosis in the presence of an external magnetic field," *Int. J. Biomath.*, vol. 4, pp. 207-225, 2011b.
[19] A. Ogulu, "Effect of heat generation on low Reynolds number fluid and mass transport in a single lymphatic vessel with uniform magnetic field," *Int. Commu. Heat and Mass Trans.*, vol. 33, pp. 790-799, 2006.
[20] A. Ogulu and E. Amos, "Modeling pulsatile blood flow within a homogeneous porous bed in the presence of a uniform magnetic field and time-dependent suction," *Int. Commun. Heat and Mass Transf.*, vol. 34, pp. 989-995, 2007.
[21] T. J. Pedley, "The fluid mechanics of large blood vessels," *Cambridge University press, Cambridge, 1980.*
[22] J. Prakash and A. Ogulu, "A study of pulsatile blood flow modeled as a Power-law fluid in a constricted tube," *Int. Commn. Heat and Mass Transfer*, vol. 34, pp. 762–768, 2007.
[23] R. N. Pralhad and D. H. Schultz, "Modelling of arterial stenosis and its applications to blood vessels," *Math. Biosc.*, vol. 19, pp. 203-220, 2004.
[24] A. R. Rao and K. S. Desikachar, "Diffusion in hydromagnetic oscillatory flow through a porous channel," *ASME J. Appl. Mech.*, vol. 54, pp. 742, 1987.
[25] G. C. Shit and M. Roy, "Pulsatile flow and heat transfer of a magneto-micropolar fluid through a stenosed artery under the influence of body acceleration," *J. Mech. Med. Biol.*, vol. 11, pp. 643-661, 2011.
[26] C. Tu and M. Deville, "Pulsatile flow of non-Newtonian fluids through arterial stenosis," *J. Biomech.*, vol. 29 pp. 899-908, 1996.
[27] C. Tu and M. Deville, L. Dheur and L. Vanderschuren, "Finite element simulation of flow through arterial stenosis," *J. Biomech.*, vol. 25, pp. 1141-1152, 1992.
[28] K. Vajravelu, K. Ramesh, S. Sreenath and P. V. Arunachalam, "Pulsatile flow between permeable beds," *Int. J. Non-Linear Mech.*, vol. 38, pp. 999-1005, 2003.
[29] M. Zamir, "Mechanics of blood supply to the heart: wave reflection effects in a right coronary artery," *Proc. R. Soc. Lond.*, vol. 26, pp. 439-444, 1998.
[30] J. R. Zierenberg, H. Fujioka, R. B. Hirschl, R. H. Bartlett and J. B. Grotberg, "Pulsatile blood flow and oxygen transport past a circular cylinder," *J. Biomech. Engg.*, vol. 129, pp. 202-215 , 2007.

ISBN: 978-988-19251-3-8
ISSN: 2078-0958 (Print); ISSN: 2078-0966 (Online)